ORIGINAL PAPER

A comparison study on interfacial properties of fluorine-bearing and fluorine-free mold flux for casting advanced high-strength steels

Jian-jun Zhang[1] · Bing-yu Zhai[2,3] · Lei Zhang[2,3] · Wan-lin Wang[2,3]

Abstract

A comparison study on interfacial properties of a traditional fluorine-bearing (F-bearing) mold flux and a newly designed fluorine-free (F-free) mold flux to produce advanced high-strength steels (AHSSs) by compact strip production technology was conducted. The results showed that these two kinds of mold fluxes gradually spread out on the typical AHSS substrate when slags began to melt with the increase in heating temperature, and they had a good interfacial ability between the two mold fluxes and the AHSS substrate, and there was no other interfacial reaction except the oxidization of steel substrate by the mold fluxes. In comparison, the wettability of the designed F-free mold flux with the AHSS substrate was better than that of the F-bearing mold flux. The reason could be explained as the addition of B_2O_3 would increase the complexity and polymerization degree of the melt structure and weaken the attractive force between the ions and ionic groups, then leading to a better wettability. Besides, B_2O_3 is an effective flux, which can reduce the melting temperature obviously, and the surface tension of the liquid F-free mold flux would get reduced with the addition of B_2O_3.

Keywords Advanced high-strength steel · Mold flux · Fluorine-free · Interfacial property · Wettability

1 Introduction

Advanced high-strength steels (AHSSs) have been developed and widely used in many fields, due to the excellent combination of high strength and ductility. To meet the huge market demand, AHSSs have recently been tried to manufacture through compact strip production (CSP), a more efficient and green continuous casting technology, which not only enhances the production efficiency and saves energies, but also refines the cast slab grain and inhibits micro-segregation. However, CSP also brings some negative effects on the process of continuous casting due to its high casting speed. CSP technology tends to introduce a random turbulence of the molten steel in the funnel-type mold and cause a large level fluctuation, which significantly increases the chance of slag entrainment [1, 2]. Then, the surface defects of slag inclusion and crack are easy to occur on the cast slab surface.

As one of the most vital metallurgical auxiliary materials in the process of continuous casting, the mold flux with excellent performances needs to be designed to tackle down above negative effects, in which the interfacial property between the liquid mold flux and initial solidification shell plays an important role [3]. Through the improvement of the interfacial property, the surface quality of slab can be effectively controlled; otherwise, those defects will develop into the slivers and blister defects in the final rolled product. Besides, the surface tension is associated with the compositions of the mold flux and steel, as well as the environmental temperatures [4]. Researches suggested that the addition of SiO_2 tends to decrease the interfacial tension, while CaO can increase the interfacial tension, because the released O^{2-} from CaO can break the bridging bonds of the Si–O slag network, leading to the depolymerization of

✉ Lei Zhang
 truth.zhang009@gmail.com

✉ Wan-lin Wang
 wanlin.wang@gmail.com

1 Central Research Institute of Baosteel (Qingshan), Wuhan 430080, Hubei, China

2 School of Metallurgy and Environment, Central South University, Changsha 410083, Hunan, China

3 National Center for International Research of Clean Metallurgy, Central South University, Changsha 410083, Hunan, China

molten structure [5]. The study of Jung et al. [6] suggested that MnO and FeO will decrease the interfacial tension, and FeO shows a stronger reduction potential on the interfacial tension than MnO. The similar result of the MnO effect on the interfacial tension was observed by Wang et al. [7]. Meanwhile, many researches have been conducted on the influence of the slag–steel reaction on the interfacial tension and wettability [8, 9].

All the above investigations focused on interfacial intension based on the traditional fluorine-bearing (F-bearing) mold flux systems. However, the fluorine in mold fluxes is easy to evaporate in the form of SiF_4 and NaF, etc., leading to the casting equipment corrosion and the environmental pollution problems [10, 11]. Therefore, many studies were conducted for the development of F-free mold flux for environment friendly and sustainable casting production, in which the effective fluxes have been tried to replace the fluorine in the traditional F-bearing mold flux, such as B_2O_3, Na_2O, and Li_2O. Previous studies [12–14] indicated that B_2O_3 is an ideal substitute for fluorine and keeps the similar physicochemical properties of traditional mold fluxes. However, there are no results published for the interfacial properties between the F-free mold flux and steel, especially for AHSS. Therefore, in this study, a B_2O_3-containing F-free mold flux was designed for the casting of a typical AHSS. And a comparison study on interfacial properties was conducted with the commercial F-bearing mold flux.

2 Experimental methods and procedure

2.1 Sample preparation

Table 1 shows the major components of a typical Si–Mn-based AHSS, which was a typical crack-sensitive medium carbon steel, and its solidus and liquidus temperatures were 1405 and 1494 °C, respectively. The steel samples were cut into a size of 50 mm (length)×50 mm (width)×4 mm (thickness) and polished by SiC sandpapers to keep a uniform surface roughness. Then, the surface roughness of the steel samples was measured by laser confocal microscopy, and the results are displayed in Fig. 1. It shows that the average surface roughness of two steel substrates is individually 9.4 and 9.5 μm, which indicates the uniform roughness is ensured for the next experiment.

Table 1 Major compositions of AHSS (mass%)

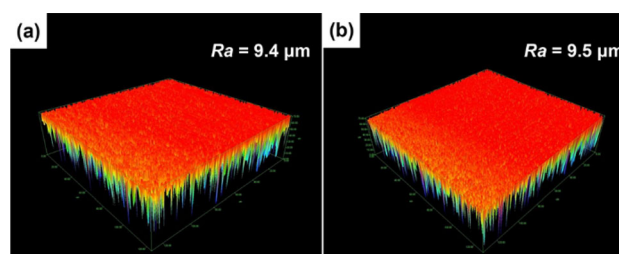| C	Si	Mn	Al	P	S	O
0.19	2.00	2.00	0.025	≤0.02	≤0.003	≤0.002

Fig. 1 Surface roughness *Ra* of AHSS substrates for two experiments. **a** F-bearing mold flux; **b** F-free mold flux

The chemical compositions of a commercial F-bearing mold flux and the designed F-free mold flux are listed in Table 2. The samples were synthesized by pure chemical reagent CaO, CaF_2, SiO_2, Al_2O_3, MgO, and B_2O_3, and heated to 1500 °C in a graphite crucible of the induction furnace for melting, and then, the sample was held for 10 min to homogenize its compositions. Next, the liquid mold flux was poured into the copper plate for air-cooling to obtain a slag disk. The slag disk was broken into half, and a part of the broken disk was subjected to a standard metallographic polishing procedure to make a cubic piece with the size of 5 mm (length)×5 mm (width)×5 mm (height). Then, the other part of the disk was crushed and ground into powders with the particle size less than 10 μm for the composition analysis, where the content of B_2O_3 was detected by inductively couple plasma (ICP), F was inspected by ion selective electrode (ISE), and the others were analyzed by X-ray fluorescence spectroscopy (XRF). The compositions of the mold fluxes after pre-melting are also listed in Table 2, suggesting that there is no obvious change in the compositions of the mold fluxes after pre-melting.

2.2 Sessile drop test

The experiments of the interfacial properties between the mold fluxes and the AHSS substrate were carried out by sessile drop apparatus, and its schematic figure is illustrated in Fig. 2, which mainly consisted of a horizontal heating furnace with high-purity alumina tube, the oxygen partial pressure control system and an image acquisition system. For the experiment, the sample mold flux cubic was firstly placed on the steel substrate, and they were pushed into the center of reaction tube. Next, the heating furnace was sealed and heated to the target temperature of 1200 °C with a fixed heating rate of 5 °C/min and held for 10 min. After that, the samples were cooled to room temperature at the cooling rate of 3 °C/min. During the whole experimental process, the tube was filled with high-purity argon gas to keep the oxygen partial pressure at $1.10×10^{-18}$ Pa for preventing the steel from oxidization. A high-resolution digital camera was applied for the in situ observation of the slag–steel interface.

Table 2 Chemical components of F-bearing and F-free mold fluxes (mass%)

Sample	Before pre-melting						After pre-melting					
							XRF				ICP	ISE
	C/S	Al_2O_3	MgO	Na_2O	B_2O_3	F	C/S	Al_2O_3	MgO	Na_2O	B_2O_3	F
F-bearing	1.25	4.00	2.00	8.00	–	10.00	1.25	4	1.98	7.88	–	9.93
F-free	1.25	4.00	2.00	8.00	6.00	–	1.25	3.9	1.99	7.90	5.50	–

C/S Ratio of mass percents of CaO and SiO_2

2.3 Analysis method for slag–steel interface

After the sessile drop test, the variation of the contact angle between the slag and steel substrate versus temperature could be analyzed by ImageJ software based on the recorded video. A typical processing procedure and the corresponding result for the contact angle between the mold flux and the AHSS substrate at 1200 °C are displayed in Fig. 3a, and then, the value of the contact angle can be obtained as shown in Fig. 3b. Then, in order to further analyze the interfacial information, the sample that the mold flux attached to AHSS substrate after sessile drop test was embedded into a resin and then subjected to scanning electron microscope (SEM, Tescan, Mira3 LMH, Czech) analysis at an accelerating voltage of 15 kV. Meanwhile, the elements distribution at the interface was analyzed by energy-dispersive spectrum (EDS).
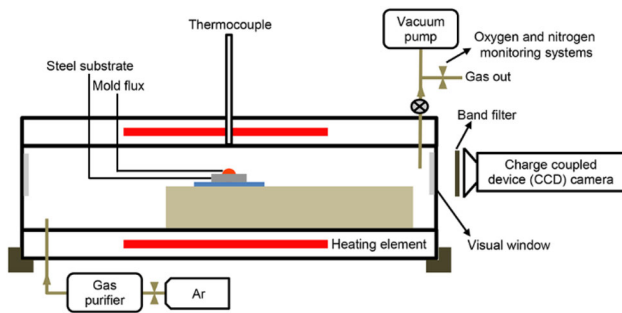

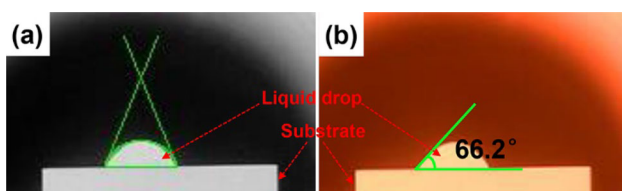**Fig. 2** Schematic of sessile drop apparatus

Fig. 3 A typical result for contact angle between mold flux and AHSS substrate at 1200 °C (**a**) and labeled diagram of contact angle (**b**)

3 Results and discussion

3.1 Interfacial behavior of mold fluxes on steel substrates

Figure 4 shows the snapshots of the morphologic variation of the two mold fluxes on the steel substrate versus heating time. Typically, the heating time can be divided into three stages. At the original stage I prior to 226 s, in which the mold flux keeps its original cubic shape on the steel substrate before melting. During stage II from 226–241 s, the slag begins to melt and gradually spread out on the steel substrate; meanwhile, the volatilization and chemical reactions may also happen. During final steady state of stage III, the shape of the liquid mold flux maintains a steady hemispheric shape on the steel substrate.

Specifically, these two kinds of mold fluxes are perpendicular to the AHSS substrate in stage I. Then, the F-free mold flux begins to melt at 1150 °C, while the F-bearing mold flux starts at 1160 °C. It suggests the melting temperature of the designed F-free mold flux is lower than that of the commercial F-bearing mold flux, and the detailed reason will be discussed in Sect. 3.3 of variation of the contact angle. During stage II, the two mold fluxes
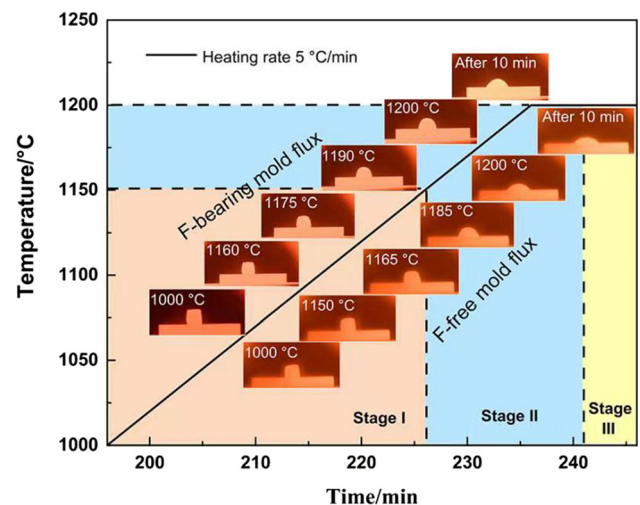

Fig. 4 Snapshots of morphologic variation of designed two mold fluxes on steel substrate versus heating time

gradually spread out and form a hemispheric shape on the steel substrate with the increase in heating temperature, and there is no visible fluctuation observed around the interface between liquid mold flux and steel substrate, indicating that there is no obvious slag–steel reaction occurring. Finally, the mold flux remains a hemispheric shape on the AHSS substrate when the temperature holds at 1200 °C in stage III. Additionally, the comparison on the variation of the contact angles for the above mold fluxes will be discussed in details in Sect. 3.3.

3.2 Observation of slag–steel interfacial microstructure

In order to further verify whether the slag–steel reactions happened or not, these two samples after sessile drop test were analyzed by SEM and EDS. Figure 5 shows the macro-morphology of the top views of the two mold fluxes, as well as their cross sections. It can be seen that there is a straight visible interfacial layer between the steel substrate and the mold flux in Fig. 5. From their cross-sectional SEM images, pores can be observed in the F-bearing mold flux, which may be due to the volatilization of fluorine. The similar phenomenon is observed by Zhao et al. [15] and Zhu et al. [16] that fluorine in mold flux volatilized in the form of NaF and SiF$_4$ at the pure argon atmosphere.

Additionally, the box I and box II at the slag–steel interface of the above two samples in Fig. 5 were further magnified and analyzed by mapping scanning of EDS, and their r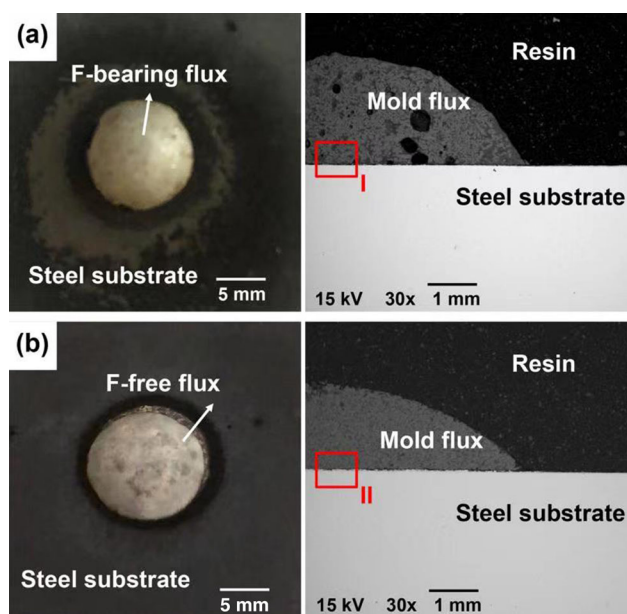esults are shown in Fig. 6, in which a thin interfacial layer between the steel substrate and mold fluxes was labeled by the dashed lines as shown in Fig. 6a and b. The thickness of the interfacial layer for the case of F-bearing mold flux is 20 μm; in comparison, it is around 50 μm for F-free mold flux, which is related to the contact angle and will be explained in Sect. 3.3. The mapping results in Fig. 6a show that Si element exists uniformly in the F-bearing mold flux; the elements of Ca, Al, Na, and F distribute in the mold flux, while O not only can be observed inside the mold flux, but also appears at the interface; besides, some amounts of Fe are observed at the interfacial layer. It is worth noting that Ca is mainly enriched in bulk, and Al and Na distribute in the matrix, the segregation of these elements occurs due to the crystallization during the cooling process with the low cooling rate of 3 °C/min.

The similar results are also observed in the case of the F-free mold flux in Fig. 6b, where O and Fe are also found at the interface. The results indicate that the interfacial layer mainly contains iron oxides, which is formed by the oxidization of the Fe in the AHSS substrate by the O in the molten slag. This is because Fe has a strong affinity for O, and there is a large concentration gradient between the mold flux and steel substrate. On the other hand, the movement of Fe atoms in steel is also promoted at the high temperature of 1200 °C, and the movement of ions and atomic group in liquid slag is more intense, which will provide a certain dynamic condition for the combination of elements in steel and slag. Thus, the combination process of the main element of Fe in AHSS substrate and the main element of O in slag will be accelerated under sufficient thermodynamic and kinetic conditions. Those results also demonstrate that there is no other slag–steel reaction except the oxidization of steel substrate by the mold fluxes, which is consistent with the results in Fig. 4.

3.3 Variation of contact angle

The contact angle of the mold fluxes can be obtained according to the method as described in Sect. 2.3 of analysis method for the slag–steel interface, and the results of the contact angle versus heating time are shown in Fig. 7. During stage I, the contact angle of the two mold fluxes maintains at 90°, as the mold fluxes keep the original solid state. With the further increase in heating time in stage II, the mold flux begins to melt, and the contact angle of F-bearing mold flux gradually decreases from 90° to 66° and then keeps relatively steady in stage III. For the case of F-free mold flux, the contact angle drops sharply from 90° to 43°, and then it also keeps a relatively steady state in stage III. The phenomenon also indicates that the wettability of the F-free mold flux on steel substrate is better than that of F-bearing mold flux, which is in accordance with the
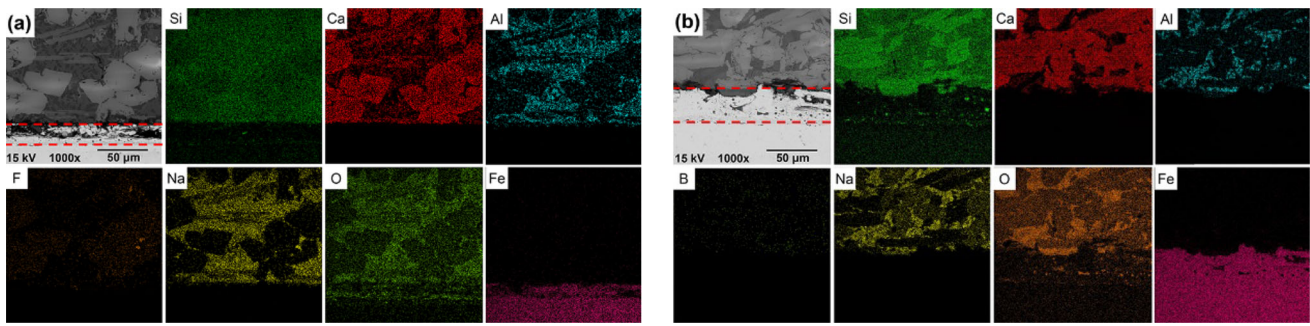

Fig. 5 Macro-morphology of top views of two mold fluxes and SEM images of their cross sections. **a** F-bearing mold flux; **b** F-free mold flux

Fig. 6 SEM images and mapping results for slag–steel interface. **a** Box I in F-bearing mold flux; **b** box II in F-free mold flux
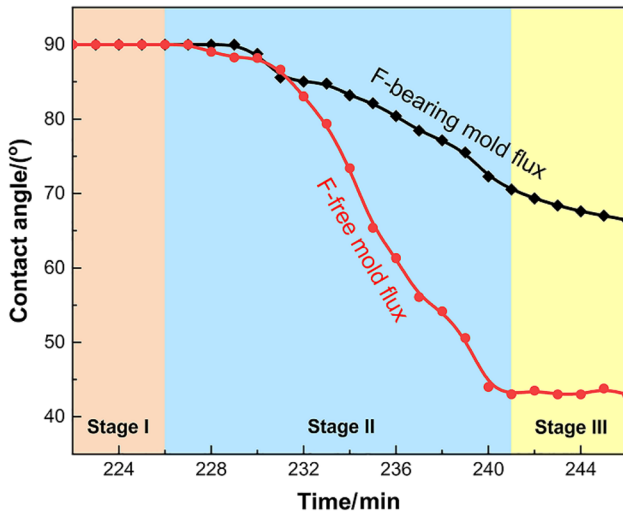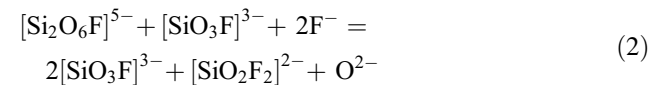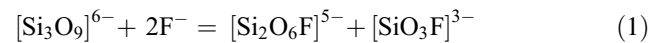

Fig. 7 Variation of contact angle between mold fluxes and steel substrates versus heating time

above results. Therefore, it explains why the interfacial layer for the case of the F-free mold flux is thicker, as the slag–metal interfacial area in this case is larger due to its better wettability. Consequently, there would be more migration of the O from mold flux and Fe from steel substrate, resulting in a thicker interfacial layer as indicated in Fig. 6, which is consistent with the findings from Bico et al. [17].

There are two main reasons for the wettability difference of the F-bearing and F-free mold fluxes on the steel substrate. First, it should be clear that the essence of interfacial tension is the intermolecular force, which is affected by attractive force and repulsive force. As the attractive force is a long-range force, it is anisotropic; the repulsive force is a short-range force and isotropic. Under the equilibrium of the two forces, the surface tension is ultimately manifested as the attractive force and the magnitude of the surface tension is also determined by the attractive force [18]. Then, a weak attractive force of the ions and ionic groups in melt surface will lead to a better wettability of molten slag on the substrate. Based on our previous studies [19, 20], B_2O_3 acts

as a typical acidic oxide in this F-free mold flux, and it can form $[BO_3]$-trihedral and $[BO_4]$-tetrahedral structural units, which introduces into the main silicate structure to form three-dimensional pentaborate complex structure, resulting in a high polymerization degree of molten slag structure, and the larger anionic groups have a weak electrostatic force on the corresponding cations. Besides, it becomes more difficult for the movement of ions and ionic groups due to the increasing molten structure complexity [21]. Thereby, their attractive force at the interface became reduced. On the contrary, Park et al. [22] reported that the fluorine in CaO–SiO_2-based slags acts as a networker breaker according to Reactions (1) and (2), the complex network structure could be depolymerized, and the polymerization degree of the melt structure would be reduced with the addition of fluorine. Therefore, the mobility of those ions and ionic groups is improved, and the force between ions and ionic groups becomes strengthened; thereby, the attractive force is enhanced.

$$[Si_3O_9]^{6-} + 2F^- = [Si_2O_6F]^{5-} + [SiO_3F]^{3-} \tag{1}$$

$$[Si_2O_6F]^{5-} + [SiO_3F]^{3-} + 2F^- = \\ 2[SiO_3F]^{3-} + [SiO_2F_2]^{2-} + O^{2-} \tag{2}$$

On the other hand, the wettability is also associated with the melting temperature of mold flux. At the same holding temperature, a lower melting temperature of mold flux means a larger superheating degree, and then a smaller contact angle will occur between the mold flux and the substrate. B_2O_3 has a stronger ability to reduce the melting point than CaF_2 in CaO–SiO_2-based slag system [23]. In the present slag system, the melting temperature of the B_2O_3-containing F-free mold flux is lower than that of the CaF_2-bearing mold flux, as shown in Fig. 4. Then, a larger superheating degree of the F-free mold flux tends to lead to the decrease in the attractive force between ions and ion clusters as the distance increases, and thus, there is a smaller contact angle between the F-free mold flux and the steel substrate. Therefore, the F-free mold flux shows a better wettability with the AHSS substrate than the F-bearing

mold flux. And the designed B_2O_3-containing F-free mold flux in the present study not only can directly avoid the pollution and harm caused by fluorine, but also effectively improve the interfacial property between slag and steel. The improvement of the interfacial property is beneficial to absorb inclusions floating from liquid steel and is also helpful to reduce the gap between the initial solidification shell and slag film to achieve uniform heat transfer. These have important reference significance for the design of environment-friendly mold flux with excellent performance, which is helpful to realize the efficient and green production of AHSS by CSP technology.

4 Conclusions

1. During the sessile drop experiments, the mold flux began to melt when the heating temperature reached the melting temperature and then spread out on the AHSS substrate. The contact angle between the mold flux and steel substrate decreased obviously with the increase in temperature after melting.

2. They had good interfacial stability between the two mold fluxes and the AHSS substrate without severe slag–metal reaction occurring. Only a thin interfacial layer about 20 μm was formed by the combination of the O element in the mold fluxes and the Fe element in the steel under sufficient thermodynamic and kinetic conditions. And the F-free mold flux showed a thicker interfacial layer about 50 μm, indicating that it has a better wettability with the AHSS.

3. The B_2O_3-containing F-free mold flux showed a better wettability, which can be attributed to the fact that B_2O_3 could combine with silicate structure to form a more complex three-dimensional melt structure, resulting in a higher polymerization degree, weakened attractive force of ions and ionic groups, and a good wettability. On the other hand, the melting temperature of the F-free mold flux was lower than that of the F-bearing mold flux, and then a larger superheating degree of the F-free mold flux could also lead to the decrease in the attractive force between ions and ion clusters in the melt.

References

[1] B.Z. Shen, H.F. Shen, B.C. Liu, ISIJ Int. 47 (2007) 427–432.
[2] Y.H. Sun, Y.J. Ni, H.T. Wang, Z.B. Xu, K.K. Cai, Int. J. Miner. Metall. Mater. 17 (2010) 159–166.
[3] S. Seetharaman, Fundamentals of metallurgy, Elsevier Press, New York, USA 2005.
[4] M. Wegener, L. Muhmood, S. Sun, A.V. Deev, Metall. Mater. Trans. B 46 (2015) 316–327.
[5] W.N. Khan, J. Kumar, R. Chhibber, Proc. Inst. Mech. Eng. Part. L. J. Mater. Des. Appl. 234 (2020) 622–636.
[6] E.J. Jung, W. Kim, I. Sohn, D.J. Min, J. Mater. Sci. 45 (2010) 2023–2029.
[7] W.L. Wang, J.W. Li, L.J. Zhou, J. Yang, Met. Mater. Int. 22 (2016) 700–706.
[8] X.B. Yan, H.Z. Yuan, S.D. Zhang, Q.Q. Wang, X.B. Zhang, S.P. He, Q. Wang, Steel. Res. Int. 91 (2020) 1900581.
[9] J.A. Yang, J.Q. Zhang, O. Ostrovski, Y. Sasaki, C. Zhang, D.X. Cai, Metall. Mater. Trans. B 50 (2019) 2175–2185.
[10] K. Shimuzu, A.W. Cramb, High. Temp. Mater. Proc. 22 (2003) 237–245.
[11] M. Persson, S. Seetharaman, S. Seetharaman, ISIJ Int. 47 (2007) 1711–1717.
[12] L.J. Zhou, W.L. Wang, J. Wei, K.C. Zhou, ISIJ Int. 55 (2015) 821–829.
[13] S. Sadaf, T. Wu, L. Zhong, Z.Y. Liao, H.C. Wang, Metals 10 (2020) 1240.
[14] A.B. Fox, K.C. Mills, D. Lever, C. Bezerra, C. Valadares, I. Unamuno, J.J. Laraudogoitia, J. Gisby, ISIJ Int. 45 (2005) 1051–1058.
[15] Z.Y. Zhao, J.X. Zhao, Z.X. Tan, B.Q. Qu, Y.R. Cui, Roy. Soc. Open. Sci. 7 (2020) 200704.
[16] L.L. Zhu, Q. Wang, S.D. Zhang, S.P. He, Z.Z. Cai, Ironmak. Steelmak. 46 (2019) 141–147.
[17] J. Bico, C. Tordeux, D. Quéré, Europhy. Let. 55 (2001) 214.
[18] A. Marchand, J.H. Weijis, J.H. Snoeijer, B. Andreotti, Am. J. Phys. 79 (2011) 999–1008.
[19] L. Zhang, W.L. Wang, S.L. Xie, K.X. Zhang, I. Sohn, J. Non-Cryst. Solids 460 (2017) 113–118.
[20] L. Zhang, W.L. Wang, I. Sohn, J. Non-Cryst. Solids 511 (2019) 41–49.
[21] K.C. Mills, ISIJ Int. 33 (1993) 148–155.
[22] J.H. Park, D.J. Min, H.S. Song, ISIJ Int. 42 (2002) 344–351.
[23] H.M. Wang, D. Fu, G.R. Li, X. Zhu, Z. Zhao, Y.T. Zhao, H. Zhu, Appl. Mech. Mater. 217–219 (2012) 511–514.